# ChemComm

## Accepted Manuscript

This article can be cited before page numbers have been issued, to do this please use: T. Liu, J. Liang, R. Xu, Y. Huang and R. Cao, *Chem. Commun.*, 2019, DOI: 10.1039/C8CC10268F.

Volume 52 | Number 1 | 4 January 2016 | Pages 1–216

ChemComm

Chemical Communications
www.rsc.org/chemcomm

ISSN 1359-7345

ROYAL SOCIETY OF CHEMISTRY

COMMUNICATION
Marilyn M. Olmstead, Alan L. Balch, Josep M. Poblet, Luis Echegoyen *et al.*
Reactivity differences of $Sc_3N@C_{2n}$ (2*n* = 68 and 80). Synthesis of the first methanofullerene derivatives of $Sc_3N@D_{5h}$-$C_{80}$

175 YEARS

ROYAL SOCIETY OF CHEMISTRY

rsc.li/chemcomm

View Article Online
DOI: 10.1039/C8CC10268F

Journal Name

COMMUNICATION

Received 00th January 20xx,
Accepted 00th January 20xx

DOI: 10.1039/x0xx00000x

www.rsc.org/

# Salen-Co(III) insertion in multivariate cationic metal-organic frameworks for the enhanced cycloaddition reaction of carbon dioxide

Tao-Tao Liu,[a,b] Jun Liang,[a] Rui-Xu,[a,b] Yuan-Biao Huang,*[a,b] and Rong Cao*[a,b]

**Salen-Co(III) motif was inserted into imidazolium-functionalized multivariate cationic zirconium metal-organic frameworks (MOFs). The salen-Co(III) as Lewis acid site while $Br^-$ of imidazolium as nucleophile is synergistically catalytic for the enhanced cycloaddition reaction of carbon dioxide with epoxides.**

As the major by-product of fossil fuel combustion, $CO_2$ is one of the culprits of the greenhouse effect that causes environmental problems including global warming, glacier retreat and frozen soil. Therefore, it is an urgent need to reduce the content of $CO_2$ in air. Compared with the adsorption method, the conversion of the adsorbed $CO_2$ into highly value-added chemicals,[1] such as cyclic carbonate,[2] is one of the most promising approaches that has the effect of two birds with one stone.

As we know, the combination of salen-Co(III) complex and co-catalyst, such as nucleophilic anion-contain imidazolium salt, has been verified to be a very effective catalytic system for promotion of cycloaddition reaction of $CO_2$ with olefin epoxides.[3] However, it is difficult to separate the product from the homogeneous catalytic system and the catalyst can't be easily recovered and reused. To circumvent these drawbacks, the incorporation of salen-Co(III) motif into porous heterogeneous catalyst containing co-catalyst is highly desired.

Porous metal-organic frameworks (MOFs)[4] constructed by metal nodes and organic linkers have shown great potential in $CO_2$ capture and heterogeneous catalysis due to their high surface area, tunable chemical and pore structures.[5] Particularly, multivariate MOFs (MTV-MOFs) containing multifunctional active sites have emerged as promising candidates for synergistic catalysis and tandem reactions.[6] Recently, the breakthrough for the synthesis of Zr-based MTV-MOFs with different length of ligands has been achieved due to the versatile connectivity and the easy formation of defect of the $Zr_6$ cluster.[7] The successful incorporation of porphyrin[8] or 1,2-bis(5-(4- carbonxyphenyl)-2-methylthien-3-yl)cyclopent-1-ene (BCDTE)[9] into UiO-66 make it possible to insert salen-M into the framework of Zr-based MOF. However, to the best of our knowledge, very rare salen-M based MTV-MOFs were reported[10] and there was no report on the salen-M incorporated into imidazolium-functionalized multivariate cationic MOF.

Herein, salen-Co(III) motif was incorporated into the framework of the imidazolium-functionalized UiO-66 via a sequential mixed-ligands synthesis and post-synthetic ionization strategy (Scheme 1). The salen-Co(III) motif as Lewis acid center and $Br^-$ of imidazolium part as nucleophile in the cationic MTV-MOF can serve as heterogeneous catalyst for the synergistically enhanced catalysis of $CO_2$ cycloaddition reaction with epoxides.

Initially, the imidazole-functionalized MTV-MOFs were synthesized from the reaction of 2-(imidazol-1-yl)terephthalic acid (Im-BDC), N,N'-Bis(3-carboxyl-salicylidene)-1,2-cyclohexanediamino cobalt(III) acetate (salen-Co(III)) with ratios of 6/4 or 9/1 and $ZrCl_4$ in DMF at 120 °C for 12 h (Scheme 1). Then, the imidazolium-functionalized cationic MTV-MOFs were obtained by the reaction of the imidazole-functionalized MTV-MOF with bromoethane. According to the inductive coupled plasma emission spectroscopy (ICP) results (Table S1), the molar ratio of the incorporated salen-Co(III) motif in all the ligands of the two cationic MTV-MOFs are 23% and 12%, respectively. So, the obtained imidazole-functionalized MTV-MOFs are denoted as Salen-Co(23%)⊂Im-UiO-66, Salen-Co(12%)⊂Im-UiO-66, while the corresponding cationic MTV-MOFs are named as Salen-Co(23%)⊂($Br^-$)Etim-UiO-66 and Salen-Co(12%)⊂($Br^-$)Etim-UiO-66, respectively. For comparison, imidazolium-functionalized cationic UiO-66 (denoted as ($Br^-$)Etim-UiO-66) was also prepared according to our previously reported method (Fig. S2).[2k] Notably, we tried to synthesize salen-Co(III) based Zr-MOF by direct synthesis method under the same conditions, however, only low crystallinity powder

---

[a] State Key Laboratory of Structural Chemistry, Fujian Institute of Research on the Structure of Matter, Chinese Academy of Sciences Fujian, Fuzhou, 350002, P.R. China. E-mail: rcao@fjirsm.ac.cn, ybhuang@fjirsm.ac.cn;
[b] University of the Chinese Academy of Sciences, Beijing, China.

† Footnotes relating to the title and/or authors should appear here.

Electronic Supplementary Information (ESI) available: [details of any supplementary information available should be included here]. See DOI: 10.1039/x0xx00000x

View Article Online
DOI: 10.1039/C8CC10268F

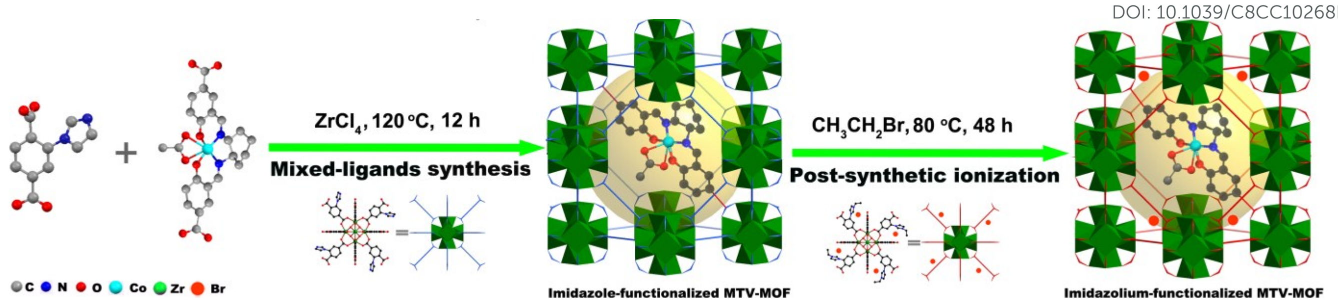

**Scheme 1** Synthesis of salen-Co(III) inserted imidazolium-functionalized MTV-MOFs by mixed-ligands synthesis and post-synthetic ionization.

was obtained (Fig. S3).

As shown in Fig. 1, the powder X-ray diffraction (PXRD) patterns of the four MTV-MOFs are consistent with those of the phase-pure UiO-66, indicating that the introduction of salen-Co(III) ligands and postsynthesis procedure did not change their topology of UiO-66. It is worth mentioning that the low crystallinity of Salen-Co(23%)⊂Im-UiO-66 and Salen-Co(23%)⊂(Br$^-$)Etim-UiO-66 revealed by the broad PXRD reflections was caused by their nanosized crystallites as shown in SEM images (Fig. 2a and Fig. S10a).[11] In the infrared spectroscopy (IR) curves (Fig. S4), the two peaks at 2939 cm$^{-1}$ and 2860 cm$^{-1}$ that attributed to the methylene in 1,2-aminocyclohexane motif were observed in the IR of the Salen-Co(23%)⊂(Br$^-$)Etim-UiO-66, indicating that salen-Co(III) has been successfully incorporated into these MTV-MOFs. The scanning electron microscopy (SEM) images show that Salen-Co(23%)⊂(Br$^-$)Etim-UiO-66 (Fig. 2a) and Salen-Co(12%)⊂(Br$^-$)Etim-UiO-66 nanocrystals (Fig. 2b) have uniform small size of about 30 nm and 100-200 nm, respectively. Such nanoscale MTV-MOFs are favorable for contacting with substrate and promoting catalysis. According to energy dispersive spectrometer (EDS) results (Table S2), the atomic content of Br in Salen-Co(23%)⊂(Br$^-$)Etim-UiO-66 and Salen-Co(12%)⊂(Br$^-$)Etim-UiO-66 are 0.44% and 1.44%, respectively, indicating that imidazolium was successfully formed. The energy-dispersive X-ray spectroscopy (EDX) mapping analysis image of Salen-Co(23%)⊂(Br$^-$)Etim-UiO-66 reveals that N, Br and Co elements are homogeneously distributed in the frameworks (Fig. 2c) suggesting that salen-Co(III) and imidazolium were uniformly grafted into the MTV-MOF.

To further confirm that whether the salen-Co(III) ligand was coordinated to the Zr$_6$ clusters framework or encapsulated in the cage of the (Br$^-$)Etim-UiO-66, N,N'-Bis(3-Br-salicylidene)-1,2-cyclohexanediamino cobalt(III) acetate (salen(Br)-Co(III)) that has the similar size with salen-Co(III) but without carboxylic acid groups, was used to replace salen-Co(III) to conduct control experiments under the same conditions. Different from light green color of salen-Co(12%)⊂(Br$^-$)Etim-UiO-66 (Fig. 2d), white powders were obtained (Fig. 2e), indicating that the ligand salen(Br)-Co(III) was not incorporated

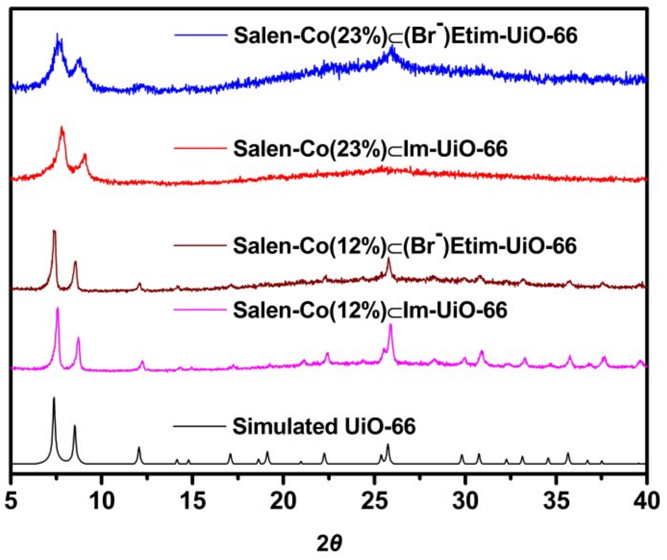

**Fig. 1** PXRD patterns of the simulated UiO-66 (black line), Salen-Co(12%)⊂Im-UiO-66 (purple line), Salen-Co(12%)⊂(Br$^-$)Etim-UiO-66 (wine red line), Salen-Co(23%)⊂Im-UiO-66 (red line) and Salen-Co(23%)⊂(Br$^-$)Etim-UiO-66 (blue line).

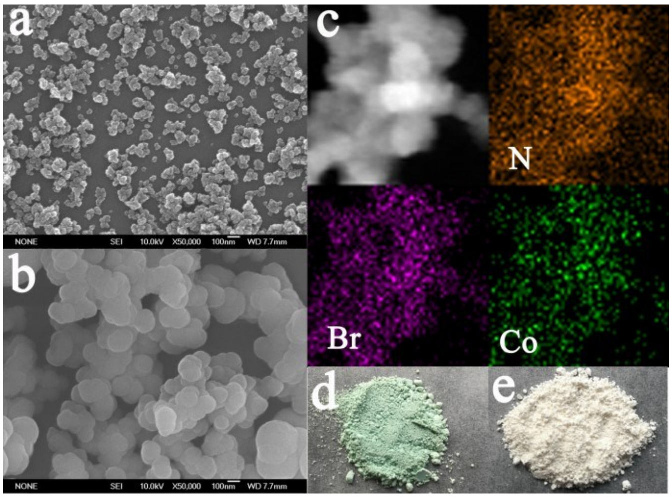

**Fig. 2** SEM images of a) Salen-Co(23%)⊂(Br$^-$)Etim-UiO-66 and b) Salen-Co(12%)⊂(Br$^-$)Etim-UiO-66 (scale bar = 100 nm), c) HAADF-STEM image and EDX elemental-mapping image (scale bar = 50nm) of Salen-Co(23%)⊂(Br$^-$)Etim-UiO-66, photographs of d) Salen-Co(12%)⊂(Br$^-$)Etim-UiO-66 and e) (Br$^-$)Etim-UiO-66 obtained from the reaction of salen(Br)-Co(III) and Im-BDC.

View Article Online
DOI: 10.1039/C8CC10268F

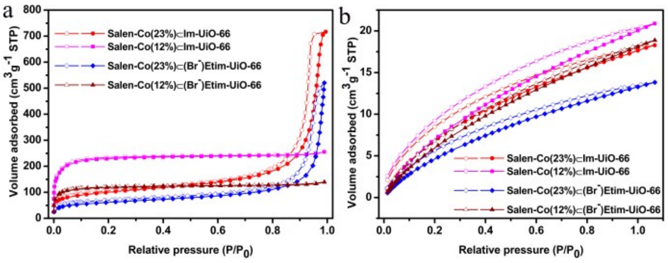

**Fig. 3** a) Nitrogen sorption curves at 77 K and b) $CO_2$ sorption curves at 298 K of the four MOFs (filled symbols for adsorption, open symbols for desorption).

in (Br$^-$)Etim-UiO-66 and highlights the importance of the carboxylic acid group, which could coordinate to the $Zr_6$ clusters.[9] More importantly, the color of the low crystallinity powder obtained from the reaction of salen-Co(III) and $ZrCl_4$ is brown (Fig. S10c) and the mixture of the low crystallinity powder and (Br$^-$)Etim-UiO-66 is light brown (Fig. S10d), proving salen-Co(III) were inserted in MTV-MOFs rather than the mixture of the low crystallinity powder and (Br$^-$)Etim-UiO-66.

Furthermore, X-ray photoelectron spectroscopy (XPS) (Fig. S6 for Co) analysis revealed that the binding energy of Co $2p_{1/2}$ and Co $2p_{3/2}$ in both salen-Co(III) ligand and Salen-Co(23%)⊂(Br$^-$)Etim-UiO-66 were 796 eV and 781 eV, respectively, indicating that the valence state of cobalt element is +3.[12] Furthermore, compared with the binding energy of N-Co (399.5 eV, Fig. S7) in salen-Co(III) ligand, the same peak in Salen-Co(23%)⊂(Br$^-$)Etim-UiO-66 was also observed. The results suggested that the salen-Co(III) motif was stable during the synthesis procedures. Such high valence state of Co(III) is favorable for activating the C-O bond of epoxides, thus could promote the cycloaddition reaction of $CO_2$.[3] Moreover, the Co-O peak (736 cm$^{-1}$, Fig. S8) of the IR of salen(Br)-Co(III) still exists under the same synthesis conditions further confirmed that Co atom could not leach from the salen-Co(III) ligand during the synthesis of MTV-MOFs. In addition, the peak at 401.5 eV of N1s in the XPS of Salen-Co(23%)⊂(Br$^-$)Etim-UiO-66 (Fig. S7b) confirmed that the successfully formation of imidazolium in the cationic MTV-MOF.

The pore features of these MTV-MOFs were tested by $N_2$ adsorption isotherms at 77 K (Fig. 3a). The curves for Salen-Co(12%)⊂Im-UiO-66 present a typical type-I behavior, indicating it is microporous material with pore sizes of 0.7 nm, 1.2 nm and 1.5 nm (Fig. S9a). Interestingly, compared with Salen-Co(12%)⊂Im-UiO-66, an obvious hysteresis desorption curve in the range of $P/P^0$ = 0.85-1 for Salen-Co(23%)⊂Im-UiO-66 is observed, indicating that macropores were formed by the interspaces of the small nanospheres. This phenomenon was coincident with the SEM image (Fig. S10a). Compared with Salen-Co(12%)⊂Im-UiO-66 with high Brunauer – Emmett – Teller (BET) surface area of 670 m$^2$g$^{-1}$, Salen-Co(23%)⊂Im-UiO-66 has a decreased BET surface area of 340 m$^2$g$^{-1}$, which was ascribed to that more pores were occupied by larger amount of salen-Co(III) motifs. The results also indicated that salen-Co(III) has been inserted in Im-UiO-66. After postsynthesis with ionization, although the imidazolium-functionalized cationic MTV-MOFs, Salen-Co(12%)⊂(Br$^-$)Etim-UiO-66 and Salen-Co(23%)⊂(Br$^-$)Etim-UiO-66, showed decreased $N_2$ adsorption uptakes compared with (Br$^-$)Etim-UiO-66 (Fig. S11) and their corresponding parent imidazole-functionalized MTV-MOFs, both of them have moderate BET surface areas of 369 m$^2$g$^{-1}$ and 208 m$^2$g$^{-1}$, respectively. Moreover, Salen-Co(12%)⊂Im-UiO-66 showed the highest $CO_2$ adsorption uptake (21 cm$^3$g$^{-1}$) among the four MTV-MOFs, which was attributed to its high BET surface area. Interestingly, although the cationic MTV-MOFs have smaller BET surface areas compared with their corresponding MOF parents, both of Salen-Co(12%)⊂(Br$^-$)Etim-UiO-66 and Salen-Co(23%)⊂(Br$^-$)Etim-UiO-66 have large $CO_2$ adsorption uptakes of 19 and 14 cm$^3$g$^{-1}$ (Fig. 3b), respectively, which is ascribed to the high $CO_2$ affinity of the imidazolium in the cationic MTV-MOFs. The high $CO_2$ adsorption of the MTV-MOFs could enhance the $CO_2$ cycloaddition reaction.

**Table 1** Synthesis of cyclic carbonates from epoxides and $CO_2$ catalyzed by Salen-Co(23%)⊂(Br$^-$)Etim-UiO-66.[a]

| Entry | Substrate | Conv / %[b] | Selec / %[b] |
|---|---|---|---|
| 1 | 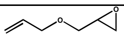 | 92 | 96 |
| 2 | 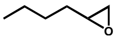 | 84 | 93 |
| 3 | 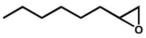 | 79 | 96 |
| 4 | 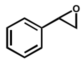 | 84 | 87 |
| 5 | 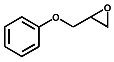 | 86 | >99 |

[a] Reaction conditions: epoxide (5 mmol), 30 mg catalyst, $CO_2$ (0.1 MPa), 393 K, 12 hours. [b] Determined by GC.

Such highly porous cationic MTV-MOFs containing salen-Co(III) Lewis acid site and imidazolium could make them as promising heterogeneous catalysts for $CO_2$ cycloaddition reactions with epoxides at 0.1 MPa without using any co-catalyst. Firstly, Salen-Co(23%)⊂(Br$^-$)Etim-UiO-66 was used as catalyst and 5 mmol allyl glycidyl ether was chosen as substrate to screen the optimized reaction conditions. At 60 $^{\circ}$C, although only 8% allyl glycidyl ether was transferred, very high selectivity for 4-allyloxymethyl-1,3-dioxolan-2-one was observed (98%, Table S3, entry 1). With the temperature increasing to 90 $^{\circ}$C, the conversion of allyl glycidyl ether increased to 44% (Table S3, entry 2). Interestingly, 92% allyl glycidyl ether can be transferred into the corresponding cyclic carbonate with 96% selectivity at 120 $^{\circ}$C within 12 h (Table S3, entry 3). Therefore, 120 $^{\circ}$C was chosen as the optimal temperature for the following catalysis. It is necessary to mention that Co cannot be detected by ICP after hot-filtration test, suggesting that the salen-Co(III) in the MOF is stable during the reaction at 120 $^{\circ}$C.

It should be noted that the reaction could not proceed without any catalyst (Table S3, entry 4). Compared with Salen-Co(23%)⊂(Br$^-$)Etim-UiO-66 with 92% selectivity, only 72% conversion was obtained when using Salen-Co(12%)⊂(Br$^-$)Etim-UiO-66 containing less amounts of salen-Co(III) sites under the same conditions (Table S3, entry 5). Furthermore,

View Article Online
DOI: 10.1039/C8CC10268F

the cationic MOF, ($Br^-$)Etim-UiO-66 containing no salen-Co(III) site exhibited only 70% conversion and 82% selectivity (Table S3, entry 6). These control experiments indicated that the incorporation of Lewis acid site salen-Co(III) in cationic MOFs indeed significantly enhanced the activity and selectivity. Besides the Lewis acid site salen-Co(III), the counterion $Br^-$ of imidaolium part also plays important role in the catalysis. Notably, the metalloligand salen-Co(III) (64% conversion and 93% selectivity, Table S3, entry 7) and Salen-Co(23%)⊂Im-UiO-66 (65% conversion and 90% selectivity, Table S3, entry 8) could catalyze the reaction due to the presence of the nucleophilic acetate ion[13] and imidazole nitrogen atoms,[14] respectively. However, compared with the bifunctional catalyst Salen-Co(23%)⊂($Br^-$)Etim-UiO-66, both of them containing no counterion $Br^-$ of imidaolium nucleophile groups showed much lower conversions and selectivities. Moreover, the physical mixture of ($Br^-$)Etim-UiO-66 and salen-Co(III) (Table S3, entry 9) showed lower catalytic activity (62% conversion and 89% selectivity), highlighting the importance of the salen-Co(III) insertion in the frameworks for the synergistically enhanced cycloaddition reaction. In addition, the bifunctional catalyst could promote transformation of a variety of long-chain and aromatic substituted epoxides, including 1,2-Epoxyhexane, 1,2-Epoxyoctane, styrene oxide, and allyl phenyl ether with satisfactory activities and selectivities (Table 1).

More importantly, the catalyst Salen-Co(23%)⊂($Br^-$)Etim-UiO-66 possesses high stability and can be easily recovered from reaction mixture by centrifugation and reused for at least five runs without significant reduction in catalytic activity (90% conversion and 96% selectivity, Fig. S12). After recycled five runs, the PXRD revealed that Salen-Co(23%)⊂($Br^-$)Etim-UiO-66 still remains UiO-66 topology (Fig. S13), although it shows reduced BET surface area (Fig. S14).

In summary, we have successfully synthesized bifunctional cationic Zr-based MTV-MOFs containing salen-Co(III) motif and imidazolium by a sequential mixed-ligands synthesis and post-synthetic ionization strategy. The amount of installed salen-Co(III) can be controllable. The cationic MTV-MOF Salen-Co(23%)⊂($Br^-$)Etim-UiO-66 was demonstrated to be highly active for the $CO_2$ cycloaddition reaction with epoxide. Moreover, it has high stability and can be recovered easily and reused at least five times without significant loss of activity.

We acknowledge the financial support from the National Key Research and Development Program of China (2018YFA0208600, 2017YFA0700100), Key Research Program of Frontier Science, CAS (QYZDJ-SSW-SLH045), Strategic Priority Research Program of the Chinese Academy of Sciences (XDB20000000), NSFC (21671188, 21871263 and 21331006), Youth Innovation Promotion Association, CAS (2014265).

## Notes and references

1 a) M. Aresta, A. Dibenedetto, and A. Angelini, *Chem. Rev.*, 2014, **114**, 1709; b) K. Paridala, S. Lu, M. Wang, C. Li, *Chem. Commun.*, 2018, **54**, 11574.

2 a) A. Decortes, A. Castilla, A. Kleij, *Angew. Chem. Int. Ed.,* 2010, **49**, 9822; b) X. Wang, X. Han, J. Zhang, X. Wu, Y. Liu, Y. Cui, *J. Am. Chem. Soc.,* 2016, **138**, 12332; c) Q. Xia, Z. Li, C. Tan, Y. Liu, W. Gong, Y. Cui, *J. Am. Chem. Soc.*, 2017, **139**, 8259; d) H. Xu, J.Hu, D. Wang, Z. Li, Q. Zhang, Y. Luo, S. Yu, H. Jiang, *J. Am. Chem. Soc.,* 2015, **137**, 13440; e) C. Gao, Q. Meng, K. Zhao, H. Yin, D. Wang, J. Guo, S. Zhao, L. Chang, M. He, Q. Li, H. Zhao, X. Huang, Y. Gao, Z. Tang, *Adv. Mater.,* 2016, **28**, 6485; f) X. Wang, Y. Zhou, Z. Guo, G. Chen, J. Li, Y. Shi, Y. Liu and J. Wang, *Chem. Sci.,* 2015, **6**, 6916; g) Q. Jiang, Z. Chen, J. Tong, M. Yang, Z. Jiang and C. Li, *ACS Catal.,* 2016, **6**, 1172; h) Z. Yang, H. Zhang, B. Yu, Y. Zhao, Z. Ma, G. Ji, B. Han and Z. Liu, *Chem. Commun.,* 2015, **51**, 11576; i) K. Wu, T. Su, D. Hao, W. Liao, Y. Zhao, W. Ren, C. Denga and H. Lü, *Chem. Commun.*, 2018, **54**, 9579; j) T. Liu, J. Liang, Y. Huang and R. Cao, *Chem. Commun.,* 2016, **52**, 13288; k) J. Liang, R. Chen, X. Wang, T. Liu, X. Wang, Y. Huang and R. Cao, *Chem. Sci.,* 2017, **8**, 1570; l) J. Liang, Y. Huang and R. Cao, *Coordin. Chem. Rev*., 2019, **378**, 32.

3 a) F. Song, C. Wang, J. Falkowski, L. Ma, and W Lin, *J. Am. Chem. Soc.,* 2010, **132**, 15390; b) H. Yang, L. Zhang, W. Su, Q. Yang and C. Li, *J. Catal*., 2007, **248**, 204.

4 a) S. James, *Chem. Soc. Rev*., 2003, **32**, 276-288; b) H. Furukawa, K. Cordova, M. Keeffe and O. Yaghi*, Science.*, 2013, **341**, 1230444; c) G. Yuan, H. Jiang, L. Zhang, Y. Liu and Y. Cui, *Coordin. Chem. Rev.,* 2019, **378**, 483; d) J. Jiao, C. Tan, Z. Li, Y. Liu, X. Han, and Y. Cui, *J. Am. Chem. Soc.,* 2018, **140**, 2251; e) C. Tan, X. Han, Z. Li, Y. Liu and Y. Cui, *J. Am. Chem. Soc.,* 2018, **140**, 16229; f) G. Yuan, Q. Zhang, Z. Wang, K. Song, X. Yuan, Y. Wang and L. Zhang, *Inorg. Chem. Front*., 2017, **4**, 764.

5 a) L. Jiao, Y. Wang, H. Jiang and Q. Xu. *Adv. Mater*., 2017, 1703663; b) C. Wu and M. Zhao, *Adv. Mater.,* 2017, **29**, 1605446; c) Y. Liu, A. Howarth, N. Vermeulen, S. Moon, J. Hupp and O. Farha, *Coordin. Chem. Rev.,* 2017, **346,** 101; d) K. Manna, P. Ji, Z. Lin, F. Greene, A. Urban, Nathan. Thacker and W. Lin, *Nat. Commun.,* 2016, **7**, 12610.

6 a) Z. Dong, Y. Sun, J. Chu, X. Zhang and H. Deng, *J. Am. Chem. Soc.,* 2017, **139**, 14209; b) Q. Liu, H. Cong and H. Deng, *J. Am. Chem. Soc.,* 2016, **138**, 13822; c) S. Yuan, W. Lu, Y. Chen, Q. Zhang, T. Liu, D. Feng, X. Wang, J. Qin and H. Zhou, *J. Am. Chem. Soc.,* 2015, **137**, 3177.

7 a) K. Manna, T. Zhang, F. Greene, and W. Lin, *J. Am. Chem. Soc.,* 2015, **137**, 2665; b) D. Feng, Z. Gu, J. Li, H. Jiang, Z. Wei, and H. Zhou, *Angew. Chem. Int. Ed.,* 2012, **51**, 10307; c) J. Cavka, S. Jacobsen, U. Olsbye, N. Guillou, C. Lamberti, S. Bordiga and K. Lillerud, *J. Am. Chem. Soc.,* 2008, **130**, 13850.

8 a) Y. Sun, L. Sun, D. Feng and H. Zhou, *Angew. Chem. Int. Ed.,* 2016, **55**, 6471; b) J. Liang, Y. Xie, Q. Wu, X. Wang, T. Liu, H. Li, Y. Huang and R. Cao, *Inorg. Chem.*, 2018, **57**, 2584.

9 J. Park, Q. Jiang, D. Feng and H. Zhou, *Angew. Chem. Int. Ed.,* 2016, **55**, 7188.

10 Q. Xia, Z. Li, C. Tan, Y. Liu, W. Gong and Y. Cui, *J. Am. Chem. Soc.,* 2017, **139**, 8259.

11 A. Schaate, P. Roy, A. Godt, J. Lippke, F. Waltz, M. Wiebcke and P. Behrens, *Chem. Eur. J.*, 2011, **17**, 6643.

12 T. Akitsu and Y. Einaga, *Polyhedron.,* 2005, **25**, 2655.

13 H. Zhang, X. Kong, C. Cao, G. Pang and Y. Shi, *J $CO_2$ Util*., 2016, **14**, 76.

14 M. Sankar, T. Ajithkumar, G. Sankar and P. Manikandan, *Catal, Commun.*, 2015, **59**, 201.